THE JOURNAL OF BIOLOGICAL CHEMISTRY VOL. 286, NO. 34, pp. 29718–29724, August 26, 2011

Oxime-assisted Acetylcholinesterase Catalytic Scavengers of Organophosphates That Resist Aging*[S]

Received for publication, May 25, 2011, and in revised form, June 30, 2011 Published, JBC Papers in Press, July 7, 2011, DOI 10.1074/jbc.M111.264739

Rory Cochran[‡], Jarosław Kalisiak[§], Tuba Küçükkılınç[‡], Zoran Radić[‡], Edzna Garcia[‡], Limin Zhang[‡], Kwok-Yiu Ho[‡], Gabriel Amitai[¶], Zrinka Kovarik[‖], Valery V. Fokin[§], K. Barry Sharpless[§], and Palmer Taylor[‡1]

From the [‡]Skaggs School of Pharmacy and Pharmaceutical Sciences, University of California, San Diego, La Jolla, California 92093-0650, the [§]Department of Chemistry and the Skaggs Institute for Chemical Biology, The Scripps Research Institute, La Jolla, California 92037, the [¶]Division of Medicinal Chemistry, Israel Institute for Biological Research, P. O. Box 19, Ness Ziona 74100, Israel, and the [‖]Institute for Medical Research and Occupational Health, P. O. Box 291, HR-10001 Zagreb, Croatia

The cholinesterases, acetylcholinesterase (AChE) and butyrylcholinesterase, are primary targets of organophosphates (OPs). Exposure to OPs can lead to serious cardiovascular complications, respiratory compromise, and death. Current therapy to combat OP poisoning involves an oxime reactivator (2-PAM, obidoxime, TMB4, or HI-6) combined with atropine and on occasion an anticonvulsant. Butyrylcholinesterase, administered in the plasma compartment as a bio-scavenger, has also shown efficacy but is limited by its strict stoichiometric scavenging, slow reactivation, and a propensity for aging. Here, we characterize 10 human (h) AChE mutants that, when coupled with an oxime, give rise to catalytic reactivation and aging resistance of the soman conjugate. With the most efficient human AChE mutant Y337A/F338A, we show enhanced reactivation rates for several OP-hAChE conjugates compared with wild-type hAChE when reactivated with HI-6 (1-(2′-hydroxyiminomethyl-1′-pyridinium)-3-(4′-carbamoyl-1-pyridinium)). In addition, we interrogated an 840-member novel oxime library for reactivation of Y337A/F338A hAChE-OP conjugates to delineate the most efficient oxime-mutant enzyme pairs for catalytic bio-scavenging. Combining the increased accessibility of the Y337A mutation to oximes within the space-impacted active center gorge with the aging resistance of the F338A mutation provides increased substrate diversity in scavenging potential for aging-prone alkyl phosphate inhibitors.

Organophosphates (OPs),[2] commonly used as pesticides, also constitute an insidious threat in terrorism and are covalent inhibitors of the cholinesterases, acetylcholinesterase (AChE) and butyrylcholinesterase (BChE) and related esterases. Human exposure to OPs results in acute poisoning manifested by salivation, tremors, respiratory paralysis, hypotension, and with more extreme exposure death (1, 2).

The efficacy of oxime therapy (typically 2-PAM, obidoxime, TMB4, or HI-6, combined with atropine and an anticonvulsant) is limited as long as inhibitory OPs remain in the different body compartments permitting redistribution into the plasma, where they are capable of inhibiting or re-inhibiting active AChE at target sites (2, 3). A newly considered treatment of acute OP intoxication therefore involves exogenous administration of BChE as a stoichiometric OP bio-scavenger efficacious in preventing full cholinesterase inhibition and death (4–6). Its limitations include a requirement for large quantities of the 80-kDa protein to scavenge stoichiometrically organophosphates of low molecular mass, sarin at 140 Da and VX at 267 Da, its propensity for aging, and a slow rate of reactivation (5–7). Recent studies have been directed at creating mutant ChE molecules circumventing these limitations (8–10). More recently, AChEs have been employed as catalytic bio-scavengers, because oxime-assisted catalysis of OP hydrolysis in the plasma compartment for bio-scavenging is expected to be reinforced by reactivation of the OP-inhibited tissue AChE by the oxime that distributes from the plasma compartment to the tissue (8, 9, 11).

A persistent and confounding complication in OP intoxication is aging of inhibited AChE, where a dealkylation step subsequent to the formation of the covalent OP-AChE conjugate yields an "aged" enzyme with an anionic phospho-conjugate unresponsive to oxime reactivation (12). Two amino acid side chains, Glu-202 and Phe-338, located close to the active Ser-203, when substituted by Gln and Ala, respectively, result in AChE mutants largely resistant to aging (13, 14).

Hence, catalytic OP turnover may be achieved by enhancing rates of oxime-assisted reactivation of ChEs by introducing side chain mutations that promote oxime attack in the active center gorge, while also yielding aging resistance, and by designing new oxime reactivators with enhanced reactivation capacities. In a recent study, a human AChE F338A mutant was characterized as an effective aging-resistant bio-scavenger of OPs (15). However, the reactivation rates for the F338A mutant enzyme are relatively slow when compared with the wild-type enzyme.

Augmenting our previous reactivation studies of mutant mouse AChE, we report on the expression and characterization of 16 human AChE mutants, 10 of which are resistant to aging.

* This work was supported, in whole or in part, by National Institutes of Health Grant U01 NS 058046 from USPHS CounterAct Program through the NINDS.

[S] The on-line version of this article (available at http://www.jbc.org) contains supplemental Figs. S1–S6, Table S1, and Movie S1.

[1] To whom correspondence should be addressed: Skaggs School of Pharmacy and Pharmaceutical Sciences, University of California, San Diego, 9500 Gilman Dr., La Jolla, CA 92093-0657. Tel.: 858-534-1366; Fax: 858-534-8248; E-mail: pwtaylor@ucsd.edu.

[2] The abbreviations used are: OP, organophosphate; AChE, acetylcholinesterase; hAChE, human AChE; ATCh, acetylthiocholine; BChE, butyrylcholinesterase; ChE, cholinesterase; 2-PAM, 2-pyridinealdoxime methiodide; HI-6, 1-(2′-hydroxyiminomethyl-1′-pyridinium)-3-(4′-carbamoyl-1-pyridinium); Flu-MPs, fluorescent methyl phosphonates; PDB, Protein Data Bank.

Our reactivation and inhibition kinetic data show that the human AChE double mutant (Y337A/F338A) is well suited to act as a non-aging, catalytic bio-scavenger. It displays faster HI-6 reactivation kinetics than wild-type human AChE for four of the five OP-AChE conjugates evaluated. To affect turnover in the plasma, alkyl phosphonylation rates in plasma must compete with the corresponding rate for organophosphate distribution in tissue. Here, we find the designed mutant enzyme retains high rates of phosphorylation by a soman analog. Finally, to provide alternatives to HI-6 and 2-PAM in the reactivation step, we describe an efficient screening method for lead oxime reactivators from a library of 840 oximes prepared largely using Cu(I)-catalyzed azide alkyne cycloaddition ("Click chemistry") to selectively obtain 1,4-disubstituted 1,2,3-triazole products.

MATERIALS AND METHODS

Organophosphates—Nonvolatile low toxicity fluorescent methyl phosphonate esters (Flu-MPs) (16) were used as analogs of the nerve agents soman, sarin, cyclosarin, and VX (supplemental Fig. S1). The Flu-MPs differ from the actual nerve agent OPs only by structure of their respective leaving groups. Inhibition of ChEs by Flu-MPs results in OP-ChE covalent conjugates identical to those formed upon inhibition with highly toxic nerve agents. The nerve agent soman was also used in some experiments. This extremely hazardous and toxic substance was handled according to safety protocols developed at the Institute for Medical Research and Occupational Health, Zagreb, Croatia. Paraoxon, an oxon of the pesticide parathion, was purchased from Sigma.

Oximes and Assay Reagents—2-PAM and HI-6 (supplemental Fig. S1) were purchased from Sigma and United States Biological (Swampscott, MA), respectively. Other oximes included in the study were synthesized by Cu(I)-catalyzed azide alkyne cycloaddition (Click chemistry) using a library of small molecule building blocks, as shown in supplemental Fig. S2. 2-PAM, HI-6, and all OPs were stored at −20 °C and diluted in water before each experiment. 5,5′-Dithiobis-(2-nitrobenzoic acid), acetylthiocholine (ATCh), and bovine serum albumin (BSA) were also purchased from Sigma.

Enzymes—Human acetylcholinesterase (hAChE) cDNA truncated at codon 547 was cloned into a pCMV-N-FLAG expression vector, obtained from Sigma. The truncated form of the enzyme results in expression of soluble monomeric enzyme, secreted into the media, as seen with murine ChE (17). The pCMV-N-FLAG vector encodes a FLAG cDNA sequence at the 5′-end of the multiple cloning site, resulting in expression of an N-terminal FLAG tag upon cleavage of the leader peptide. cDNAs encoding mutant hAChEs were prepared using site-directed mutagenesis by overlap extension PCR (18) with Phusion DNA polymerase obtained from New England Biolabs (Ipswich, MA). Double and triple hAChE mutants were prepared using sequence-confirmed single and double mutant cDNAs, respectively, as templates in subsequent PCRs.

HEK-293 cells, obtained from American Type Culture Collection (Manassas, VA), were transfected with hAChE expression vectors using conventional calcium phosphate transfection. Stable neomycin-resistant clones were selected for and isolated using G418 from Invitrogen. hAChE was harvested from liter quantities of media in quantities of several milligrams and purified using immunoaffinity chromatography with anti-FLAG affinity resin from Sigma. Coomassie staining was used to assess purity.

Kinetic Experiments—AChE activity was measured using the Ellman assay (17) at room temperature in 0.1 M sodium phosphate buffer, pH 7.4, containing 333 μM 5,5′-dithiobis-(2-nitrobenzoic acid), 0.01% BSA, typically at 1.0 mM substrate ATCh concentration. hAChE-OPs were generated by incubating enzyme with at least a 4-fold molar excess of OP for 5–30 min until inhibition exceeded 95%. hAChE-OPs were passed through a Sephadex G-50 spin column to remove excess inhibitor and subsequently diluted. Control samples were treated similarly but lacked the addition of OP. Determination of enzyme kinetic parameters, inhibition, and reactivation constants were carried out as described previously (8, 19, 20).

Selection of Candidate Oximes from a Compound Library—Oxime selections were carried out by measuring AChE activity using the Ellman assay with 1 mM ATCh. A library of 700 Click chemistry crude reaction mixtures containing mostly the desired triazole product (supplemental Fig. S2) and a library of 140 purified oximes (data not shown) were screened in a 96-well format by measuring the percent reactivation after either 10- or 60-min incubation periods at 37 °C with 0.67 mM oxime. Incubation periods of reactivation were based on reactivation rates of 2-PAM and HI-6 for each of the studied enzymes. Because oxime reactivators generally act as reversible AChE inhibitors, dual controls, in the presence and absence of oxime, were assayed in separate wells for each of screened reactivators. Oximes showing pronounced (≥50%) reversible inhibition in control measurements were re-examined at lower oxime concentrations, according to the procedure shown in supplemental Fig. S3.

Computational Molecular Modeling—Interaction of HI-6 and the active center gorge of VX-inhibited hAChE was studied for the WT and Y337A/F338A mutant using a simulated annealing molecular dynamics approach (21). Covalent conjugates of *O*-ethyl methylphosphonylated AChE at the active Ser-203 were generated by pasting *O*-ethyl methylphosphonylated Ser-203 of mouse AChE structure (PDB code 2JGH) into the native WT hAChE structure (PDB code 3LII) and subsequent semi-empirical quantum mechanical adjustment of partial charges by InsightII suite (Accelrys, San Diego). A model of the double hAChE mutant Y337A/F338A was created by deleting all heavy side chain atoms of Tyr-337 and Phe-338 except for Cα and Cβ. All water molecules were removed from the PDB structures and a dielectric constant of 4 was used to mimic the interior of the hAChE active center gorge. The identical HI-6 conformation used to start both WT and mutant calculations was extracted from PDB code 2GYU. In all calculations, the distance between oximate oxygen of HI-6 and the phosphorus atom of VX conjugates was additionally flexibly constrained to a distance between 0 and 3.00 Å. Ten calculations were made for both the WT and mutant HI-6·hAChE complexes leaving the HI-6 molecule and hAChE residues 72, 124, 286, 295, 297, 337, 338, 341, and 447 free to rotate although all other enzyme residues were immobilized.

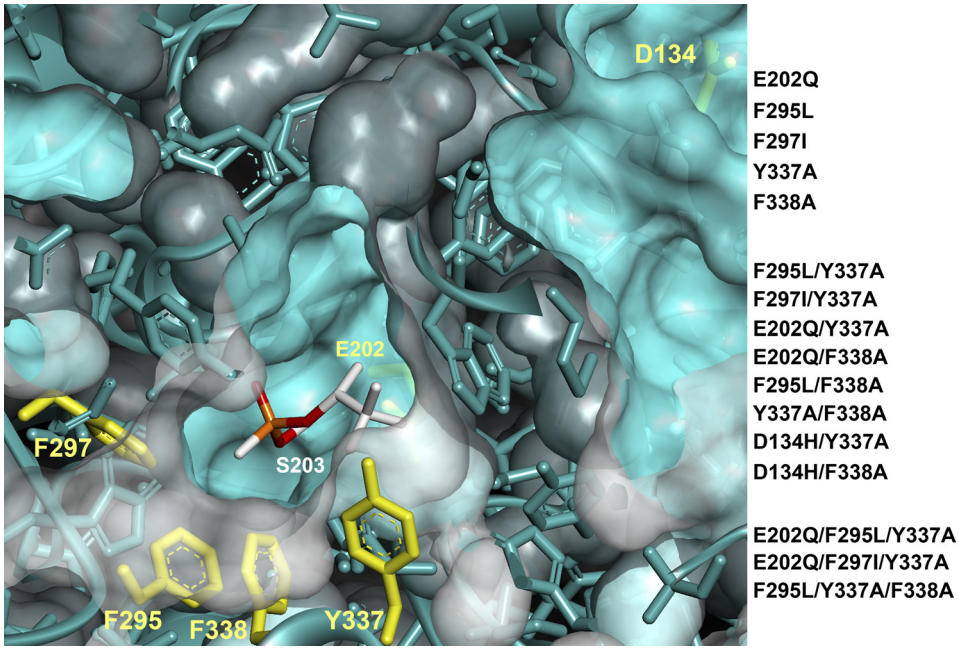

FIGURE 1. **Mutants of human AChE created and tested in this study.** Mutated residues in the active center gorge of hAChE (PDB code 3LII) are highlighted in *yellow*. Non-aged soman conjugate attached to the active Ser-203 rendered in *white* (C), *orange* (P), and *red* (O) sticks is overlaid into hAChE from the soman inhibited *Torpedo californica* AChE structure (PDB code 2WG2).

RESULTS

Human AChE Mutant Permutations—Human AChE acyl pocket and choline-binding site mutants were designed from previous findings establishing that certain mouse AChE mutants improved HI-6-elicited reactivation rates of OP-AChE conjugates (8, 9). In particular, we generated aging-resistant bio-scavengers for treatment of intoxication by soman, an OP exhibiting rapid aging of its OP-hAChE covalent conjugate (22). Thus, we created 16 different single, double, and triple mutants (Fig. 1).

Catalytic Activity—Catalytic parameters for ATCh hydrolysis catalyzed by the mutants are shown in Table 1. As seen previously, mutations in the choline-binding site did not shift the K_m value dramatically from the wild-type value (23). However, in the acyl pocket, single mutants F295L and F297I shifted the K_m and K_{ss} values to higher substrate concentrations. Not surprisingly, the acyl pocket/choline-binding site double mutants (F295L/Y337A, F297I/Y337A, and F295L/F338A) exhibited large shifts in their K_m and K_{ss} constants. The double mutant, Y337A/F338A at the choline-binding site displayed simple Michaelis-Menten kinetics devoid of substrate inhibition, as indicated by $b = 1$ (supplemental Fig. S4). The naturally occurring human AChE single nucleotide polymorphism, D134H (24), when combined with the choline-binding site mutations (Y337A and F338A), did not exhibit different kinetic characteristics from the corresponding single mutants. As noted previously, mutations outside of the active center gorge could affect catalysis through long range interactions (25).

Reactivation of OP-hAChE Conjugates—To identify suitable AChE oxime pairs for catalytic bio-scavenging, reactivation rates for each mutant OP-hAChE conjugate were determined using HI-6 and 2-PAM (supplemental Fig. S1). The fluorescent soman congener was the lead OP. Only 2 of 10 mutants, E202Q/Y337A and Y337A/F338A (Table 2; Fig. 2; and supplemental Fig. S5), showed rapid reactivation without appreciable aging. However, reactivation kinetics showed that the favorable second order rate constant exhibited by the E202Q/Y337A mutant arose from a low K_{ox} value but with relatively slow turnover (small k_{max}). In contrast, the soman-Y337A/F338A conjugate exhibited more promising kinetic characteristics when reactivated with HI-6 (Fig. 2; supplemental Fig. S5). Very similar reactivation kinetics were obtained when, instead of PMP-MeCyc, a fluorescent-MP analog (supplemental Fig. S1) nerve agent, soman itself was used to prepare *O*-pinacolyl methylphosphonyl OP-hAChE conjugate of Y337A/F338A mutant (Table 2).

TABLE 1

Catalytic constants for ATCh hydrolysis by wild type and mutant human AChE in 0.1 M phosphate buffer, pH 7.4, at 22 °C

For all studied enzymes, inhibition by excess ATCh was evident except for F297I/Y337A and Y337A/F338A, where ATCh hydrolysis followed simple Michaelis kinetics ($b = 1$). Hydrolysis by F295L/Y337A/F338A was activated by excess substrate ($b > 1$). k_{cat} values for WT hAChE and mutants F338A and Y337A/F338A were determined as $(1.4 \pm 0.40)\cdot10^5$ min^{-1}, $(0.74 \pm 0.21)\cdot10^5$ min^{-1}, and $(0.53 \pm 0.09)\cdot10^5$ min^{-1}, respectively.

hAChE	K_m	K_{ss}	b
	(μM)	(mM)	
WT	160 ± 12	10 ± 1	0.097 ± 0.019
E202Q	370 ± 20	64 ± 19	0.24 ± 0.08
F295L	530 ± 54	43 ± 13	0.17 ± 0.08
F297I	2800 ± 170	240 ± 25	0
Y337A	130 ± 10	6.9 ± 1.5	0.54 ± 0.02
F338A	180 ± 23	3.0 ± 0.8	0.42 ± 0.03
F295L/Y337A	710 ± 31	420 ± 45	0
F297I/Y337A	4000 ± 140		1.0
E202Q/F338A	670 ± 300	4.1 ± 3.8	0.46 ± 0.13
E202Q/Y337A	200 ± 20	7.7 ± 2.5	0.53 ± 0.03
F295L/F338A	350 ± 18	110 ± 7	0
Y337A/F338A	270 ± 18		1.0
D134H/Y337A	270 ± 27	7.5 ± 2.1	0.51 ± 0.02
D134H/F338A	310 ± 21	6.0 ± 1.1	0.52 ± 0.02
E202Q/F295L/Y337A	360 ± 26	25 ± 6	0.39 ± 0.03
E202Q/F297I/Y337A	610 ± 38	660 ± 140	0
F295L/Y337A/F338A	1700 ± 250	44 ± 8	3.00 ± 0.21

This indicates that neither the use of a nerve agent surrogate nor amino acid substitutions altered the stereospecificity of formation of the OP-Y337A/F338A conjugate and that enhancements of reactivation kinetics refer to the most reactive soman diastereoisomer (P_SC_S) inducing the fastest AChE aging (26).

TABLE 2

Comparison of second order reactivation rate constants (k_r), maximal reactivation rate constants (k_{max}), Michaelis-type constants (K_{ox}), and the final amount of recovered activity (percent of uninhibited control) for reactivation of soman-inhibited hAChE mutants, with HI-6 in 0.1 M phosphate buffer, pH 7.4, at 22 °C

hAChE-mutant	K_{ox}	k_{max}	k_r	Recovery
	μM	min^{-1}	$M^{-1}\ min^{-1}$	%
F338A	81 ± 34	0.027 ± 0.002	330 ± 130	19–64
F295L/F338A	45 ± 18	0.024 ± 0.002	520 ± 180	9–33
E202Q/Y337A	28 ± 11	0.057 ± 0.004	2000 ± 650	40–81
Y337A/F338A	400 ± 99	1.0 ± 0.1	2500 ± 520	28–70
Y337A/F338A[a]	550 ± 290	1.1 ± 0.3	2100 ± 1200	65–95

[a] Inhibited enzyme was prepared using soman nerve agent instead of the soman fluorescent-MP analog *O*-pinacolyl O-(3-cyano-4-methyl-7-coumarin) methyl phosphonate.

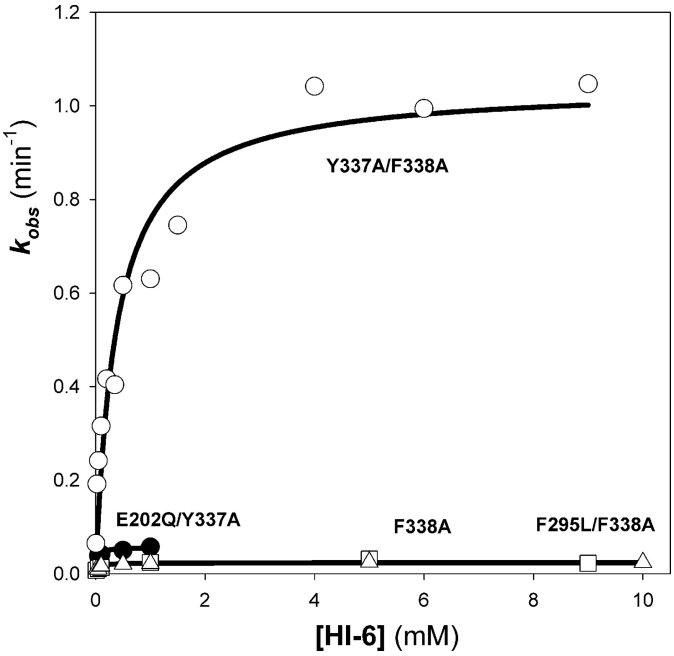

FIGURE 2. **Reactivation kinetics of soman-inhibited human AChE mutants refractory to aging, by HI-6.** Reactivation constants determined by nonlinear regression of data for human AChE mutants F338A (*squares*), E202Q/Y337A (*black circles*), F295L/F338A (*triangles*), and Y337A/F338A (*white circles*) in 0.1 M phosphate buffer, pH 7.4, at 22 °C are given in Table 3.

Because the remaining double and triple mutants displayed very slow reactivation rates for most of the OP inhibitors in question (data not shown), further characterization was not pursued.

Non-aging Catalytic Bio-scavenger—Consistent with recent findings indicating that the single hAChE F338A mutant is an aging-resistant bio-scavenger (15), we sought to optimize reactivation rates through suitable mutant AChE-oxime pairs. Indeed, the hAChE Y337A/F338A mutant showed increased reactivation rates for several OP-enzyme conjugates when reactivated with HI-6 (Table 3). The reactivation for three *O*-alkyl methyl phosphonates of three nerve agent conjugates (VX, sarin, and soman) was enhanced compared with the wild-type enzyme. In addition, a substantial increase in the reactivation rate for the paraoxon-AChE, a phosphate conjugate, was seen for this double mutant as well (Table 3; supplemental Fig. S6).

The most notable improvement in reactivation kinetics was observed with the VX-AChE conjugate. The second order rate constant, k_r, was approximately 1 order of magnitude larger than the wild-type enzyme (Table 3; supplemental Fig. S6). Importantly, the K_{ox} constants for the double mutant with each of the assayed inhibitors remained comparable with the wild-type values, demonstrating that the OP-conjugated mutant AChE retains its binding affinity toward the oxime reactivator.

We further analyzed the kinetics of the Y337A/F338A hAChE inhibition with the fluorescent soman analog (supplemental Fig. S1) to ensure that the two engineered mutations did not reduce inhibition rates to a degree that would alter the rate-limiting step in the overall inhibition/reactivation scheme. As seen in Table 4, the second order inhibition rate constant, k_i, for the Y337A/F338A hAChE was not reduced (9.4×10^5 *versus* $7.9 \times 10^5\ M^{-1}\ min^{-1}$ for WT hAChE); however, the maximal inhibition rate reflected in the k_2 constant was substantially lower. This should not diminish the capacity for this mutant AChE as a catalytic bio-scavenger because inhibition rate constants for OP conjugation are 2 orders of magnitude or more greater than reactivation rate constants. Hence, the dephosphorylation step should be rate-limiting in the catalytic scavenging of soman and other *O*-alkyl methyl phosphonates.

Consistent with kinetic data, computational molecular modeling indicated that relieving congestion in the active center of the OP-hAChE conjugate by substituting two large aromatic side chains (Tyr-337 and Phe-338) with alanine facilitated HI-6 binding close to the phosphorus atom (average distances

TABLE 3

Reactivation kinetics for OP-inhibited human AChE wild type and Y337A/F338A mutant with HI-6

The second order reactivation rate constants (k_r), maximal reactivation rate constants (k_{max}), and Michaelis-type constants (K_{ox}) for reactivation were performed in 0.1 M phosphate buffer, pH 7.4, at 22 °C.

OP	hAChE	K_{ox}	k_{max}	k_r	k_r^{mut}/k_r^{wt}
		μM	min^{-1}	$M^{-1}\ min^{-1}$	
Soman	WT	ND[a]	ND	ND	≫1
	Y337A/F338A	400 ± 99	1.00 ± 0.06	2500 ± 520	
VX	WT	240 ± 0.05	0.61 ± 0.05	2500 ± 410	10
	Y337A/F338A	130 ± 17	3.20 ± 0.17	26000 ± 2500	
Sarin	WT	150 ± 100	0.66 ± 0.12	4400 ± 2400	1.8
	Y337A/F338A	150 ± 24	1.20 ± 0.05	7900 ± 980	
Cyclosarin	WT	440 ± 90	6.8 ± 0.6	15000 ± 2000	0.42
	Y337A/F338A	240 ± 70	1.50 ± 0.13	6300 ± 1300	
Paraoxon	WT	540 ± 110	0.022 ± 0.002	41 ± 5	6.6
	Y337A/F338A	190 ± 80	0.05 ± 0.006	270 ± 90	

[a] ND means not detected due to fast aging of WT hAChE upon inhibition by soman.

between HI-6 oximate and VX phosphorus were 5.4 ± 0.6 and 3.7 ± 0.1 Å in the WT VX-hAChE and the Y337A/F338A conjugate, respectively), while allowing the HI-6 oximate more conformational flexibility in the angle of approach to the phosphorus atom (Fig. 3 and supplemental Movie S1).

Selection of Candidate Oximes from a Compound Library— In addition to our mutagenesis studies, we investigated 840 novel oximes to examine their capacity to assist the dephosphorylation step with the aging-resistant mutant. A majority of the compounds were synthesized using Cu(I)-catalyzed azide alkyne cycloaddition (Click chemistry), a biorthogonal reaction between an acetylenic and azide building blocks containing an appropriate oxime functionality to form triazoles. Nearly quantitative cycloaddition efficiency of Click chemistry allowed us to screen compounds directly from synthetic reaction mixtures conducted in multiwell plates (27).

Initially, a library of 140 purified compounds (data not shown) was screened for their ability to reactivate the WT and the Y337A/F338A double mutant OP conjugates as diagramed in supplemental Fig. S3. Subsequently, we tested ~700 nonpurified Click chemistry reaction mixtures formed in small quantities in the arrays. The feasibility of using nonpurified mixtures in the reactivation screen was demonstrated by parallel reactivation of 10 of the purified oxime compounds (five strong and five weak reactivators) and their corresponding nonpurified Click chemistry reaction mixtures where little or no difference was observed.

Scoring candidate reactivator compounds based on percent recovery of enzyme activity for the corresponding OP-AChE conjugate after a given time period or an end point absorbance reading (Fig. 4) enabled us to dismiss hundreds of compounds with very small or no reactivating capacity. In addition, we established an internal control to determine the degree of reversible inhibition by oximes for native hAChE or mutant using hAChE that were not exposed to OPs (Fig. 4). Reactivation of several oximes identified as strong reversible inhibitors of hAChE were examined again at 5–10-fold lower oxime concentrations.

Upon screening all 840 candidate oximes, we were unable to find reactivators with reactivation kinetics better than HI-6 for the nerve agent analogs assayed (Fig. 4). However, several compounds that exhibited the capacity to reactivate certain OP-AChE conjugates faster than 2-PAM were identified (supplemental Table S1). The best reactivating agent for recovery of paraoxon-inhibited enzyme is shown in Table 5. Interestingly, two of the three oximes identified with improved reactivation kinetics over 2-PAM were imidazolium derivatives (supplemental Table S1).

TABLE 4

Comparison of inhibition kinetics for human AChE wild-type enzyme and Y337A/F338A mutant with *O*-pinacolyl O-(3-cyano-4-methyl-7-coumarin) methyl phosphonate (soman fluorescent-MP analog) in 0.1 M phosphate buffer, pH 7.4, at 22 °C

hAChE	k_i ($\times 10^5$ M^{-1} min^{-1})	K_i	k_2
		μM	min^{-1}
WT	7.9 ± 1.4	5.0 ± 2.3	3.9 ± 1.2
F338A	1.9 ± 0.5	4.8 ± 2.2	0.9 ± 0.2
Y337A/F338A	9.4 ± 1.3	0.38 ± 0.1	0.36 ± 0.02

DISCUSSION

Because of recent incidents of chemical terrorism and the ease of synthesis of toxic OPs, increased attention has been accorded to developing improved prophylactic and antidotal therapy. Current treatment for acute OP toxicity is limited by the effectiveness of BChE as a bio-scavenger and by the absence of efficient oximes that are applicable across a wide range of inhibitors. Consequently, efforts to engineer catalytic AChE bio-scavengers and generate improved oxime reactivators have continued over the last decade (28). Within this framework, soman presents a particular enigma, because it must be hydrolyzed or detoxified in the plasma before it is distributed to the tissues where it reacts with the target and immediate AChE aging ensues. In this study, we sought to design AChE mutants that would not only act catalytically to turn over the OP in the presence of an oxime but have non-aging properties as well. We designed 10 AChE mutants that were expected to confer aging resistance by virtue of mutations localized to the Glu-202 and Phe-338 positions. In addition, based on our previous studies

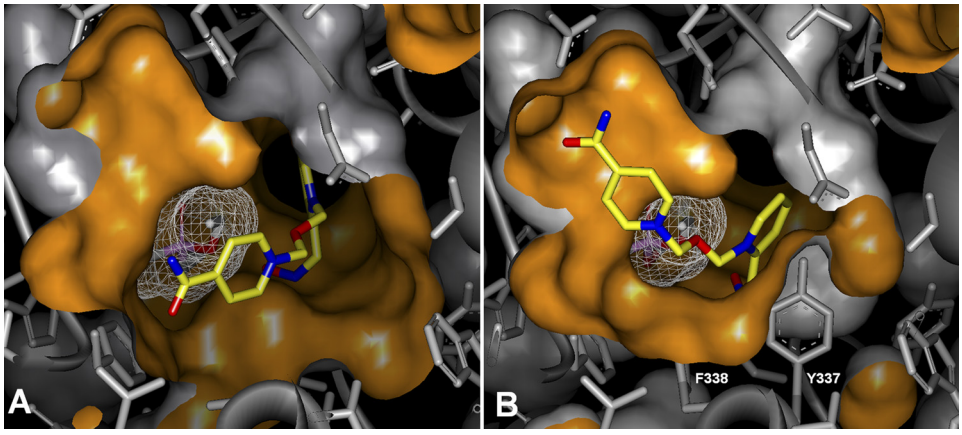

FIGURE 3. **Computational models of HI-6 docked into the active center gorge of Y337A/F338A VX-hAChE (*A*) and WT VX-hAChE (*B*) (using InsightII Discover by Accelrys, San Diego) reveal respective average distances (from 10 calculations) between HI-6 oximate oxygen and VX phosphorus to be 5.4 ± 0.6 and 3.7 ± 0.1 Å suggesting easier access of the nucleophilic oximate of HI-6 to the phosphorus atom of VX in the wider active center gorge of the Y337A/F338A hAChE mutant resulting in acceleration of the reactivation reaction.** The interior of the AChE active center is represented by *orange* solvent-accessible surface; the outer side of the surface is colored *gray*; the *white mesh* represents solvent-accessible surface of the VX conjugate with the active Ser-203. HI-6 is represented as *yellow* (C), *blue* (N), and *red* (O) sticks.

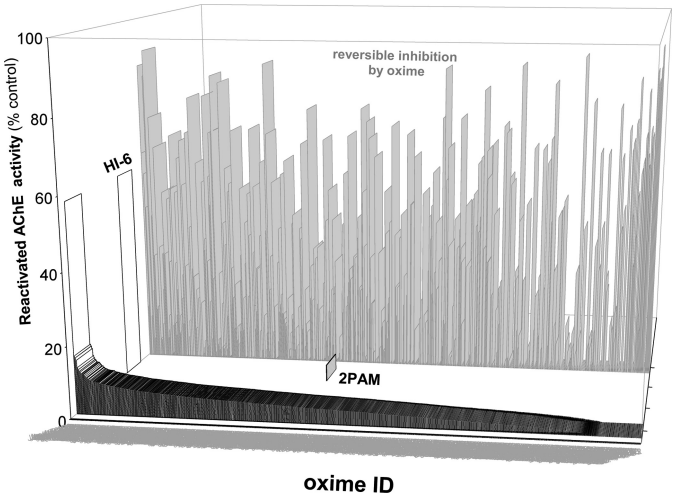

FIGURE 4. **Profile for reactivation of soman-inhibited Y337A/F338A hAChE upon 10 min of incubation with the library of 840 oximes (0.67 mM in 0.1 M phosphate buffer, pH 7.4, at 37 °C).** Reactivated hAChE activity was measured by continuous activity assay (Δ*A*/min) at 412 nm and compared with HI-6 and 2-PAM recovered activity indicated by separate *white* and *gray bars*. Percent of hAChE inhibition by 6.7 μM oximes seen in the activity assay in the presence of 1.0 mM ATCh is also shown (*light gray bars* in the background).

TABLE 5

Top ranking oxime candidate for human AChE Y337A/F338A mutant inhibited with paraoxon

Reactivation constants were in 0.1 M phosphate buffer, pH 7.4, at 37 °C.

Oxime	K_{ox} (μM)	k_{max} (min^{-1})	k_r ($M^{-1}min^{-1}$)	Structure
177	120 ± 30	1.00 ± 0.07	8500	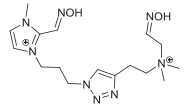
2-PAM	1600 ± 130	0.24 ± 0.01	150	

with mouse AChE, we engineered mutations within the acyl pocket and choline-binding site, because mutations localized within these regions yielded improved reactivation rates with HI-6 for specific inhibitors (8, 9).

Shafferman *et al.* (14) have examined aging kinetics for a series of mutations around the active center gorge of AChE and recognized anionic residues that enhance the potential of stabilizing a presumed carbonium ion intermediate in the aging reaction (29). This might occur through charge neutralization by ionizable side chains or through forming cation-quadrupole interactions with aromatic side chains. Eliminating charge neutralization (mutants E202N and E450N) or aromaticity in the vicinity of the active center (Y338A) serves to diminish rates of aging (13, 14). Hence, in our double mutant, the Y338A mutation confers resistance to the spontaneous aging reaction and the neighboring Y337A mutation allows for deeper penetration of oxime to the conjugated phosphorus (supplemental Movie S1). This is achieved in the double mutant without appreciable compromise of the rate of formation of the alkyl phosphate conjugate.

Curiously, we found several kinetic differences between the corresponding murine and human AChE mutants. The largest differences were seen in their reactivation rates with HI-6. In our previous work, we observed a marked enhancement in reactivation rates with the F295L/Y337A AChE mutant over that of WT mouse AChE (8); however, in this study we did not observe an analogous enhancement with the corresponding mutations in hAChE. Although HI-6 reactivation kinetics were significantly slower for WT mouse AChE than for WT human AChE for the cyclosarin methyl phosphonate (mAChE $k_r = 112$ M^{-1} min^{-1}; hAChE $k_r = 15{,}000$ M^{-1} min^{-1}), the lower fractional enhancement for hAChE brings the two F295L/Y337A AChE mutants into a similar range (mAChE F295L/Y337A $k_r = 13{,}180$ M^{-1} min^{-1}) (8). Furthermore, human AChE enzymes with either acyl pocket mutation (F295L or F297I) alone showed minimal enhancements in reactivation rates. We observed that consistent with this trend, as more modifications were made to the active center gorge as seen in the triple mutants, large decreases in kinetic constants, inhibition, and reactivation rates became evident. Studies with human AChE would be preferred in therapy because an endogenous protein with the mutations buried deep in the gorge can be expected to minimize immunogenicity with subsequent AChE treatments.

Of the 16 human AChE mutants characterized, only one showed the kinetic promiscuity to be considered universally reactive among the organophosphate conjugates studied to date. The human AChE Y337A/F338A mutant displayed ideal reactivation kinetics to act as a non-aging catalytic bio-scavenger. The double mutant displayed enhanced reactivation rates over the wild-type enzyme for four (soman, sarin, VX, and paraoxon) of the five OPs evaluated. Consistent with our previous work, the Y337A mutation conferred enhanced reactivation with HI-6. However, the moiety was dependent upon synergy with the F338A mutation, as the single mutants alone yielded only minimal enhancements. Similar to a previous study of the F338A single mutant (15), the Y337A/F338A mutant showed promising reactivation rates when inhibited with soman, an OP well known for causing fast aging. Much to our excitement, the Y337A/F338A double mutant displayed faster reactivation kinetics than the single F338A mutant alone when inhibited with soman. Molecular modeling suggests that a facilitated approach of HI-6 in the immediate vicinity to the phosphorus and increased freedom of attack angles upon decongestion of the impacted active center (by removal of two aromatic side chains) are consistent with lower K_{ox} values obtained for the large soman conjugate of the double mutant and larger k_{max} values observed for VX, sarin, and paraoxon conjugates. Our findings suggest that the Y337A/F338A mutant might be particularly effective at ameliorating current therapeutic shortcomings of BChE for certain OPs prone to cause OP-AChE aging. However, pharmacokinetic studies to prolong lifetimes in the plasma (30, 31) will be needed to evaluate the ability of hAChE to improve protection against OP toxicity *in vivo*. Nonetheless, the Y337A/F338A double mutant in the presence of an oxime should be considered as a viable candidate for replacement of BChE.

Complementing our efforts to improve upon current bioscavenging approaches, we carried out exhaustive drug screening experiments to find nucleophiles with improved reactivation potential. Using our sequential screening procedure involving an initial rapid screen followed by developing kinetic curves on selected leads, we were able to identify several lead

compounds from a library of ~840 oxime compounds with an improved capacity to reactivate both the wild type and Y337A/F338A enzymes when inhibited with paraoxon. We were unable, however, to find any lead oximes with enhanced capacity over HI-6 and 2-PAM to reactivate the nerve agent-inhibited enzymes. Nonetheless, some of the lead compounds exceeded 2-PAM in promoting turnover. The structures of the lead compounds (and the failures) provide new insights into what components are required for reactivating potential and to furnish information for further systematic design of prophylactic and therapeutic reactivating agents. Finally, novel approaches to synthesis and selection of leads has enhanced our efficiency for surveying compounds for reactivation of AChE or BChE.

Acknowledgment—The assistance of Wenru Yu in expression and purification of recombinant hAChE and mutants is greatly appreciated.

REFERENCES

1. Taylor, P. (2011) in *Goodman & Gilman's The Pharmacological Basis of Therapeutics* (Brunton L. L., Chabner, B., and Knollman, B., eds) 13th Ed., pp. 239–254, McGraw-Hill Inc., New York
2. Croddy, E., and Wirtz, J. J. (eds) (2005) *Weapons of Mass Destruction: An Encyclopedia of Worldwide Policy, Technology, and History*, pp. 1–449, ABC-CLIO, Greenwood, Santa Barbara, CA
3. McDonough, J. H., and Romano, J. A., Jr. (2007) *Chemical Warfare Agents: Chemistry, Pharmacology, Toxicology, and Therapeutics* (Romano, J. A., Lukey, B. J., and Salem, H., eds) 2nd Ed., pp. 71–96, CRC Press, Inc., Boca Raton, FL
4. Cerasoli, D. M., Griffiths, E. M., Doctor, B. P., Saxena, A., Fedorko, J. M., Greig, N. H., Yu, Q. S., Huang, Y., Wilgus, H., Karatzas, C. N., Koplovitz, I., and Lenz, D. E. (2005) *Chem. Biol. Interact.* **157–158,** 363–365
5. Raveh, L., Grauer, E., Grunwald, J., Cohen, E., and Ashani, Y. (1997) *Toxicol. Appl. Pharmacol.* **145,** 43–53
6. Raveh, L., Grunwald, J., Marcus, D., Papier, Y., Cohen, E., and Ashani, Y. (1993) *Biochem. Pharmacol.* **45,** 2465–2474
7. Wolfe, A. D., Blick, D. W., Murphy, M. R., Miller, S. A., Gentry, M. K., Hartgraves, S. L., and Doctor, B. P. (1992) *Toxicol. Appl. Pharmacol.* **117,** 189–193
8. Kovarik, Z., Radić, Z., Berman, H. A., Simeon-Rudolf, V., Reiner, E., and Taylor, P. (2004) *Biochemistry* **43,** 3222–3229
9. Kovarik, Z., Radić, Z., Berman, H. A., and Taylor, P. (2007) *Toxicology* **233,** 79–84
10. Saxena, A., Maxwell, D. M., Quinn, D. M., Radić, Z., Taylor, P., and Doctor, B. P. (1997) *Biochem. Pharmacol.* **54,** 269–274
11. Taylor, P., Kovarik, Z., Reiner, E., and Radić, Z. (2007) *Toxicology* **233,** 70–78
12. Fleisher, J. H., and Harris, L. W. (1965) *Biochem. Pharmacol.* **14,** 641–650
13. Saxena, A., Doctor, B. P., Maxwell, D. M., Lenz, D. E., Radic, Z., and Taylor, P. (1993) *Biochem. Biophys. Res. Commun.* **197,** 343–349
14. Shafferman, A., Ordentlich, A., Barak, D., Stein, D., Ariel, N., and Velan, B. (1996) *Biochem. J.* **318,** 833–840
15. Mazor, O., Cohen, O., Kronman, C., Raveh, L., Stein, D., Ordentlich, A., and Shafferman, A. (2008) *Mol. Pharmacol.* **74,** 755–763
16. Amitai, G., Adani, R., Yacov, G., Yishay, S., Teitlboim, S., Tveria, L., Limanovich, O., Kushnir, M., and Meshulam, H. (2007) *Toxicology* **233,** 187–198
17. Ellman, G. L., Courtney, K. D., Andres, V., Jr., and Featherstone, R. M. (1961) *Biochem. Pharmacol.* **7,** 88–95
18. Ho, S. N., Hunt, H. D., Horton, R. M., Pullen, J. K., and Pease, L. R. (1989) *Gene* **77,** 51–59
19. Kovarik, Z., Radić, Z., Berman, H. A., Simeon-Rudolf, V., Reiner, E., and Taylor, P. (2003) *Biochem. J.* **373,** 33–40
20. Radić, Z., Gibney, G., Kawamoto, S., MacPhee-Quigley, K., Bongiorno, C., and Taylor, P. (1992) *Biochemistry* **31,** 9760–9767
21. Ashani, Y., Radić, Z., Tsigelny, I., Vellom, D. C., Pickering, N. A., Quinn, D. M., Doctor, B. P., and Taylor, P. (1995) *J. Biol. Chem.* **270,** 6370–6380
22. Froede, H. C., and Wilson, I. B. (1971) in *The Enzymes* (Boyer, P. D., ed) 3rd Ed., Vol. 5, p. 87, Academic Press, New York
23. Ordentlich, A., Barak, D., Kronman, C., Flashner, Y., Leitner, M., Segall, Y., Ariel, N., Cohen, S., Velan, B., and Shafferman, A. (1993) *J. Biol. Chem.* **268,** 17083–17095
24. Valle, A. M., Radić, Z., Rana, B. K., Mahboubi, V., Wessel, J., Shih, P. A., Rao, F., O'Connor, D. T., and Taylor, P. (2011) *J. Pharm. Exp. Ther.* **338,** 125–133
25. Küçükkilinç, T., Cochran, R., Kalisiak, J., Garcia, E., Valle, A., Amitai, G., Radiæ, Z., and Taylor, P. (2010) *Chem. Biol. Interact.* **187,** 238–240
26. Ordentlich, A., Barak, D., Kronman, C., Benschop, H. P., De Jong, L. P., Ariel, N., Barak, R., Segall, Y., Velan, B., and Shafferman, A. (1999) *Biochemistry* **38,** 3055–3066
27. Kolb, H. C., Finn, M. G., and Sharpless, K. B. (2001) *Angew. Chem. Int. Ed. Engl.* **40,** 2004–2021
28. Taylor, P., Reiner, E., Kovarik, Z., and Radiæ, Z. (2007) *Arh Hig Rada Toksikol.* **58,** 339–345
29. Aldridge, W. N., and Reiner, E. (1972) *Enzyme Inhibitors as Substrates. Interactions of Esterases with Esters of Organophosphorous and Carbamic Acids,* pp. 1–328, North-Holland Publishing Co., Amsterdam
30. Huang, Y. J., Lundy, P. M., Lazaris, A., Huang, Y., Baldassarre, H., Wang, B., Turcotte, C., Côté, M., Bellemare, A., Bilodeau, A. S., Brouillard, S., Touati, M., Herskovits, P., Bégin, I., Neveu, N., Brochu, E., Pierson, J., Hockley, D. K., Cerasoli, D. M., Lenz, D. E., Wilgus, H., Karatzas, C. N., and Langermann, S. (2008) *BMC Biotechnol.* **8,** 50
31. Rosenberg, Y. J., Saxena, A., Sun, W., Jiang, X., Chilukuri, N., Luo, C., Doctor, B. P., and Lee, K. D. (2010) *Chem. Biol. Interact.* **187,** 279–286